

• 基础研究 •

两种小鼠模型在胆汁淤积性肝损伤实验中的应用

路寒¹, 张雪飞¹, 孙学伟², 张若男³, 张昕蕊⁴, 张明燕⁵, 唐成亮², 杨展², 朱进², 杨晓俊^{1*}

¹南京医科大学第二附属医院普外科, 江苏 南京 210003; ²东部战区疾病预防控制中心传染病防控二科, 江苏 南京 210002; ³南京医科大学病原生物学系, 江苏 南京 211166; ⁴南京中医药大学医学院整合医学学院, ⁵金陵临床医学院, 江苏 南京 210046

[摘要] 目的: 比较胆管结扎(bile duct ligation, BDL)和 α -萘基异硫氰酸酯(α -naphthylisothiocyanate, ANIT)诱导的胆汁淤积性肝损伤小鼠模型的差异, 探讨两种模型在胆汁淤积性肝损伤实验中的应用范围。方法: 将C57BL/6小鼠随机分为对照组、假手术组(Sham组)、BDL组、BDL+短链脂肪酸(short-chain fatty acid, SCFA)组、ANIT组和ANIT+SCFA组。BDL组、BDL+SCFA组在第1天进行BDL手术, ANIT组和ANIT+SCFA组在第1天开始通过灌胃方式给予100 mg/kg ANIT, 每周1次, BDL+SCFA组和ANIT+SCFA组自造模日起, 持续14 d自由饮用含SCFA的水(67.5 mmol/L乙酸钠、25.9 mmol/L丙酸钠、40 mmol/L丁酸钠), 共观察14 d。收集各组小鼠肝组织以及血清样本后, 通过苏木精-伊红(hematoxylin and eosin, HE)染色评估肝脏病理变化, 采用生化试剂盒检测血清丙氨酸氨基转移酶(alanine aminotransferase, ALT)、天冬氨酸氨基转移酶(aspartate aminotransferase, AST)、碱性磷酸酶(alkaline phosphatase, ALP)和总胆红素(total bilirubin, TBIL)水平, 并通过ELISA测定白细胞介素(interleukin, IL)-6、IL-1 β 、单核细胞趋化蛋白-1(monocyte chemoattractant protein-1, MCP-1)水平。结果: BDL组小鼠早期(第1周)出现明显黄疸和持续体重下降, 后期(第2周)出现严重黄疸。ANIT组小鼠早期表现为轻度黄疸和体重下降, 后期黄疸逐步加深。两种模型的肝组织大体与形态学中存在共同表现: 肝脏硬化、肝细胞坏死、汇管区纤维化、炎症细胞浸润以及胆管增生。但BDL组早期出现上述表现且较重, 而ANIT组早期表现较轻但后期加重。血清学指标显示, 两组小鼠肝脏转氨酶水平均明显上升(P 均 < 0.05); BDL组早期ALP和TBIL水平较对照组显著升高($P < 0.05$), 较ANIT组升高明显($P < 0.05$), ANIT组小鼠的ALP和TBIL水平早期仅轻度升高, 后期逐步升高($P < 0.05$)。血清炎症因子分析显示, BDL组小鼠早期IL-1 β 、IL-6和MCP-1水平显著高于对照组($P < 0.05$), 而ANIT组小鼠的炎症因子水平早期仅轻度上升, 后期逐步升高并接近BDL组水平($P > 0.05$)。SCFA治疗对BDL组小鼠的黄疸、体重下降、血清肝功能指标(ALT、AST、ALP和TBIL)及炎症因子水平(IL-6和MCP-1)均无显著改善($P > 0.05$)。然而, 在ANIT组小鼠中, SCFA治疗显著改善黄疸和体重下降($P < 0.05$), 并降低ALT、AST、TBIL水平($P < 0.05$)。此外, SCFA干预后ANIT组小鼠的IL-1 β 、IL-6和MCP-1水平明显降低($P < 0.05$)。结论: BDL模型具有起病急、肝损伤严重的特点, 适合研究急性胆汁淤积性肝损伤, ANIT模型表现为起病缓慢、肝损伤逐渐加重, 更适合模拟慢性胆汁淤积性肝损伤。

[关键词] 胆汁淤积性肝损伤; 胆管结扎; α -萘基异硫氰酸酯; 短链脂肪酸

[中图分类号] R575

[文献标志码] A

[文章编号] 1007-4368(2025)05-627-10

doi: 10.7655/NYDXBNSN250096

The application of two mouse models in cholestatic liver injury experiments

LU Han¹, ZHANG Xuefei¹, SUN Xuewei², ZHANG Ruonan³, ZHANG Xinrui⁴, ZHANG Mingyan⁵, TANG Chengliang², YANG Zhan², ZHU Jin², YANG Xiaojun^{1*}

¹Department of General Surgery, the Second Affiliated Hospital of Nanjing Medical University, Nanjing 210003;

²Infectious Disease Prevention and Control Division II, Eastern Theater Disease Prevention and Control Center,

Nanjing 210002; ³Department of Pathogen Biology, Nanjing Medical University, Nanjing 211166; ⁴School of

Integrative Medicine, ⁵Jinling Clinical Medical College, Nanjing University of Traditional Chinese Medicine, Nanjing

210046, China

[Abstract] **Objective:** To compare the differences between two mouse models of cholestatic liver injury induced by bile duct ligation

[基金项目] 伊犁哈萨克自治州科研计划项目(YJC2023A27); 伊犁临床医学研究院科研课题(y12023ms07)

*通信作者(Corresponding author), E-mail: yangxiaojunvip@163.com (ORCID: 0000-0001-8873-3652)

(BDL) and α -naphthylisothiocyanate (ANIT) respectively, and to explore the applicability of these models in cholestatic liver injury research. **Methods:** Male C57BL/6 mice were randomly divided into six groups: control, sham, BDL, BDL+short-chain fatty acid (SCFA), ANIT, and ANIT+SCFA groups. BDL and BDL+SCFA groups underwent BDL surgery on day 1, while ANIT and ANIT+SCFA groups were administered 100 mg/kg ANIT *via* gavage weekly starting from day 1 to induce liver injury, BDL+SCFA and ANIT+SCFA groups received water containing SCFA (67.5 mmol/L sodium acetate, 25.9 mmol/L sodium propionate, and 40 mmol/L sodium butyrate) for 14 days. After the collection of liver tissues and serum samples from mice of each group, liver histopathology was assessed by hematoxylin and eosin (HE) staining. Serum levels of alanine aminotransferase (ALT), aspartate aminotransferase (AST), alkaline phosphatase (ALP), and total bilirubin (TBIL) were measured using biochemical assay kits, while the concentrations of inflammatory cytokines interleukin (IL)-6, IL-1 β , and monocyte chemoattractant protein-1 (MCP-1) were determined by ELISA. **Results:** Mice in the BDL group exhibited marked jaundice and continuous weight loss within the first week, progressing to severe jaundice by the second week. In contrast, the ANIT group displayed mild jaundice in the early stage, which gradually worsened, with only slight initial weight loss and minimal subsequent change. Both models shared common gross and histopathological features, including partial hepatic cirrhosis, hepatocellular necrosis, portal fibrosis, inflammatory cell infiltration, and bile duct proliferation. However, these features appeared earlier and were more pronounced in the BDL group, whereas the ANIT group showed milder early changes that progressively intensified as the study progressed. Serum biochemical analysis revealed significant elevations in hepatic transaminase levels in both groups ($P < 0.05$). In the BDL group, early ALP and TBIL levels were significantly higher than those in the control group ($P < 0.05$) and markedly exceeded those in the ANIT group ($P < 0.05$). In the ANIT group, ALP and TBIL levels were only mildly elevated in the early stage but gradually increased in later stage ($P < 0.05$). Analysis of serum inflammatory cytokines showed that IL-1 β , IL-6, and MCP-1 levels were significantly higher in the BDL group than in the control group in the early stage ($P < 0.05$), while in the ANIT group, cytokine levels increased only slightly at first and then gradually rose to levels comparable to those of the BDL group by the later stages ($P > 0.05$). After two weeks of SCFA treatment, no significant improvement was observed in jaundice, weight loss, serum liver function markers (ALT, AST, ALP, and TBIL), or inflammatory cytokine levels (IL-6 and MCP-1) in the BDL group ($P > 0.05$). Conversely, SCFA treatment in the ANIT group significantly alleviated jaundice and weight loss ($P < 0.05$) and reduced ALT, AST, and TBIL levels ($P < 0.05$). Furthermore, SCFA intervention markedly decreased IL-1 β , IL-6, and MCP-1 levels in the ANIT group ($P < 0.05$). **Conclusion:** The BDL model, characterized by rapid onset and severe liver injury, is suitable for studying acute cholestatic liver injury, whereas the ANIT model, with its gradual onset and progressively worsening liver damage, is more appropriate for simulating chronic cholestatic liver injury.

[Key words] cholestatic liver injury; bile duct ligation; α -naphthylisothiocyanate; short-chain fatty acids

[J Nanjing Med Univ, 2025, 45(05):627-636]

胆汁淤积性肝损伤是指由于胆汁生成或排泄功能受损引起的胆汁淤积和毒性胆酸蓄积的一类疾病,随病程进展可导致肝纤维化甚至终末期肝病^[1-2]。胆汁淤积的病因复杂多样,包括肝内胆汁淤积,如妊娠期胆汁淤积、病毒性肝炎、药物性肝损伤、酒精性肝病、原发性胆汁性肝硬化(primary biliary cholangitis, PBC)和原发性硬化性胆管炎(primary sclerosing cholangitis, PSC)等^[3-4];肝外胆汁淤积,如胆总管结石、胰管癌和胆道闭锁等^[5]。胆汁淤积性肝损伤发病率在世界范围内呈上升趋势^[6],而目前治疗手段有限^[7-8]。为研究胆汁淤积性肝损伤的发病机制,探索新的治疗药物及方法,目前发明众多动物模型,其中常用两种小鼠胆汁淤积性肝损伤模型——胆管结扎(bile duct ligation, BDL)和 α -萘基异硫氰酸酯(α -naphthylisothiocyanate, ANIT)诱导模

型,分别代表了机械性和化学性病因素导致的胆汁淤积性肝损伤^[9]。

BDL模型通过手术部分或全部阻断肝外胆管,造成胆汁流出受阻,从而引发急性胆汁淤积、胆管细胞增生及显著的纤维化反应^[10]。该模型主要表现为肝外胆道梗阻,重复性高,实验周期短,已被广泛应用于研究胆汁淤积导致的肝脏形态和功能改变,如胆管细胞增殖、纤维化形成^[11-13]。

ANIT作为一种由肝细胞代谢后进入胆汁的毒性物质,通过化学性损伤作用于肝内胆管细胞,诱导胆管细胞坏死,促进胆管增生和炎症反应,最终导致肝纤维化^[14]。ANIT模型肝外胆管大多不受影响,主要作用于肝内胆管,与人类自身免疫性胆汁淤积性疾病(如PSC)在某些病理特征上较为相似^[15]。

短链脂肪酸(short-chain fatty acid, SCFA)是肠

道微生物发酵膳食纤维的代谢产物,具有抗炎、抗氧化、抗纤维化等作用^[16-19]。本课题组前期研究证明SCFA可缓解对乙酰氨基酚诱导的急性肝损伤^[20]。本研究对BDL模型与ANIT模型导致的胆汁淤积肝损伤相关指标进行比较,并使用SCFA作为治疗药物,观察两种模型肝损伤的缓解情况,以揭示两种模型在胆汁淤积性肝损伤实验中的应用区别。

1 材料和方法

1.1 材料

1.1.1 动物

8~10周龄SPF级C57BL/6雄性小鼠(北京斯贝福生物有限公司)。小鼠在动物房内自由饮食,环境设置为12h光照/黑暗循环,温度控制在23℃,湿度控制在53%。本研究经南京医科大学第二附属医院医学伦理委员会审批(审批号2022KY05801),所有动物实验均按照实验动物护理和使用指南进行。

1.1.2 试剂

α -萘基异硫氰酸酯(Sigma-Aldrich公司,美国),橄榄油、乙酸钠、丙酸钠和丁酸钠(上海生物工程),血清谷丙转氨酶(alanine aminotransferase, ALT)、谷草转氨酶(aspartate aminotransferase, AST)、总胆红素(total bilirubin, TBIL)及碱性磷酸酶(alkaline phosphatase, ALP)检测试剂盒(南京建成),ELISA检测试剂盒(南京拉普达)。

1.2 方法

1.2.1 动物模型构建及分组

适应性喂养1周后,小鼠被随机分至对照组、假手术(sham)组、BDL组、BDL+SCFA组、ANIT组和ANIT+SCFA组,每组12只。BDL组和BDL+SCFA组小鼠依照文献^[11]进行BDL手术,即沿腹中线打开腹部,进入腹腔,用棉签沾湿生理盐水提起肝脏,将胆管从门静脉和肝动脉旁分离出来,用4-0缝合线2次结扎,但不解剖胆管,以避免胆汁泄漏。用生理盐水冲洗腹腔,将腹部器官恢复至生理位置,随后关闭腹部,观察14d;Sham组只开腹,不结扎胆管;ANIT组和ANIT+SCFA组小鼠灌胃给药ANIT(100 mg/kg,溶于橄榄油),每周1次,观察14d;BDL+SCFA组和ANIT+SCFA组小鼠在造模后提供含SCFA(67.5 mmol/L乙酸钠、25.9 mmol/L丙酸钠、40 mmol/L丁酸钠)的水,自由饮用14d;对照组正常喂养,未特殊处理。在实验进行第7天处死对照组、Sham组、BDL组、ANIT组小鼠各6只,第14天处死剩余所有小鼠,收集肝脏和血液。血液3 500 r/min

离心15 min,将血清分离,将血清及部分肝脏组织冻存于-80℃冰箱待测。

1.2.2 血清学指标检测

本研究采用南京建成生物工程有限公司提供的比色试剂盒对血清中ALT、AST、ALP和TBIL水平进行检测。此外,针对细胞因子白细胞介素-6(interleukin-6, IL-6)、白细胞介素-1 β (interleukin-1 β , IL-1 β)和单核细胞趋化蛋白-1(monocyte chemoattractant protein-1, MCP-1)的检测,使用南京拉普达ELISA试剂盒通过固相化抗体捕获目标分子,结合酶标记二抗进行信号放大,最终通过450 nm波长下吸光度值与重组标准曲线的比对实现定量分析。

1.2.3 HE染色

将新鲜的肝脏组织浸泡在4%多聚甲醛中,固定24 h,石蜡包埋,切成5 μ m厚的切片,二甲苯脱蜡,无水乙醇水合,HE染色固定,镜下观察肝脏组织形态变化。参考Ishak分级系统^[21]对纤维化分期进行判定,扩展以下半定量评分(0~4分):①汇管区纤维化,0分为无纤维化;1分为部分汇管区纤维性扩展,伴或不伴短纤维间隔;2分为大部分汇管区纤维性扩展,伴短纤维间隔;3分为汇管区纤维扩展伴偶发汇管-汇管(P-P)桥接;4分为显著桥接纤维化(P-P和/或汇管-中央静脉桥接)或早期结节形成(不完全肝硬化)。②炎症细胞浸润,0分为无浸润;1分为轻度,部分或全部汇管区可见少量淋巴细胞浸润;2分为中度,部分或全部汇管区可见中等量淋巴细胞浸润;3分为中-重度,全部汇管区可见密集淋巴细胞浸润;4分为重度,全部汇管区可见显著密集淋巴细胞浸润伴滤泡形成。③胆管增生,0分为无增生;1分为轻微增生;2分为轻度增生;3分为中度增生;4分为重度或结节性增生。④坏死结节,0分为无坏死;1分为微小坏死灶;2分为局灶性坏死;3分为多灶融合坏死;4分为大片坏死。

1.3 统计学方法

使用GraphPad Prism 10软件进行数据分析。各组数据以均数 \pm 标准差($\bar{x} \pm s$)表示,组间比较采用单因素方差分析(one-way ANOVA),若ANOVA结果显示显著性差异($P < 0.05$),进一步使用Tukey多重比较检验分析具体组间差异。 $P < 0.05$ 为差异有统计学意义。

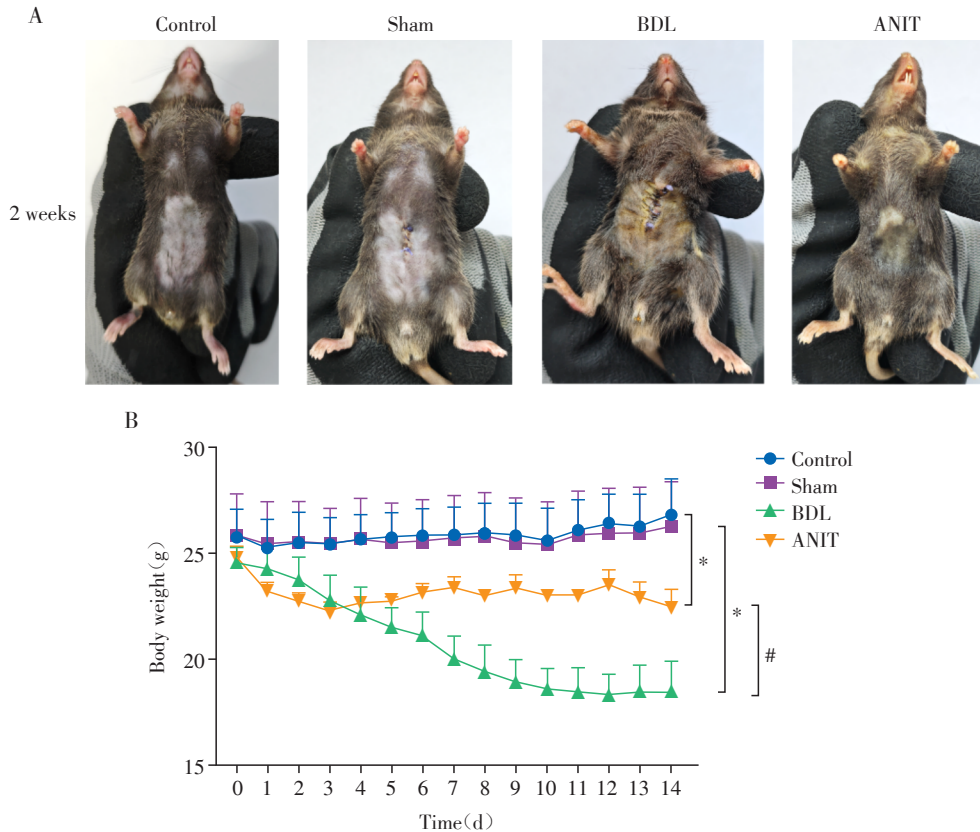
2 结果

2.1 两种模型小鼠的外观表现对比

本研究建立了两种常用的胆汁淤积小鼠模

型: BDL模型和 ANIT模型。BDL组的小鼠早期(1周)出现黄疸,精神状态差,毛发无光泽、易脱落,尿液呈深黄色,体重持续下降明显,且较 ANIT组下降更显著($P < 0.05$),后期(2周)出现

严重黄疸, ANIT组的小鼠早期出现轻微黄疸,但持续加重,精神不佳,毛发无光泽;体重早期下降,后期变化不明显,较对照组有显著差异($P < 0.05$, 图1A、B)。



A: Changes in the appearance of mice were observed two weeks after model induction. B: Body weight changes in mice from different groups. Compared to the control or sham group, * $P < 0.05$; compared to the ANIT group, # $P < 0.05$ ($n=6$).

图1 各组小鼠外观与体重表现

Figure 1 Appearance and body weight changes in mice of different groups

2.2 两种小鼠模型的肝损伤对比

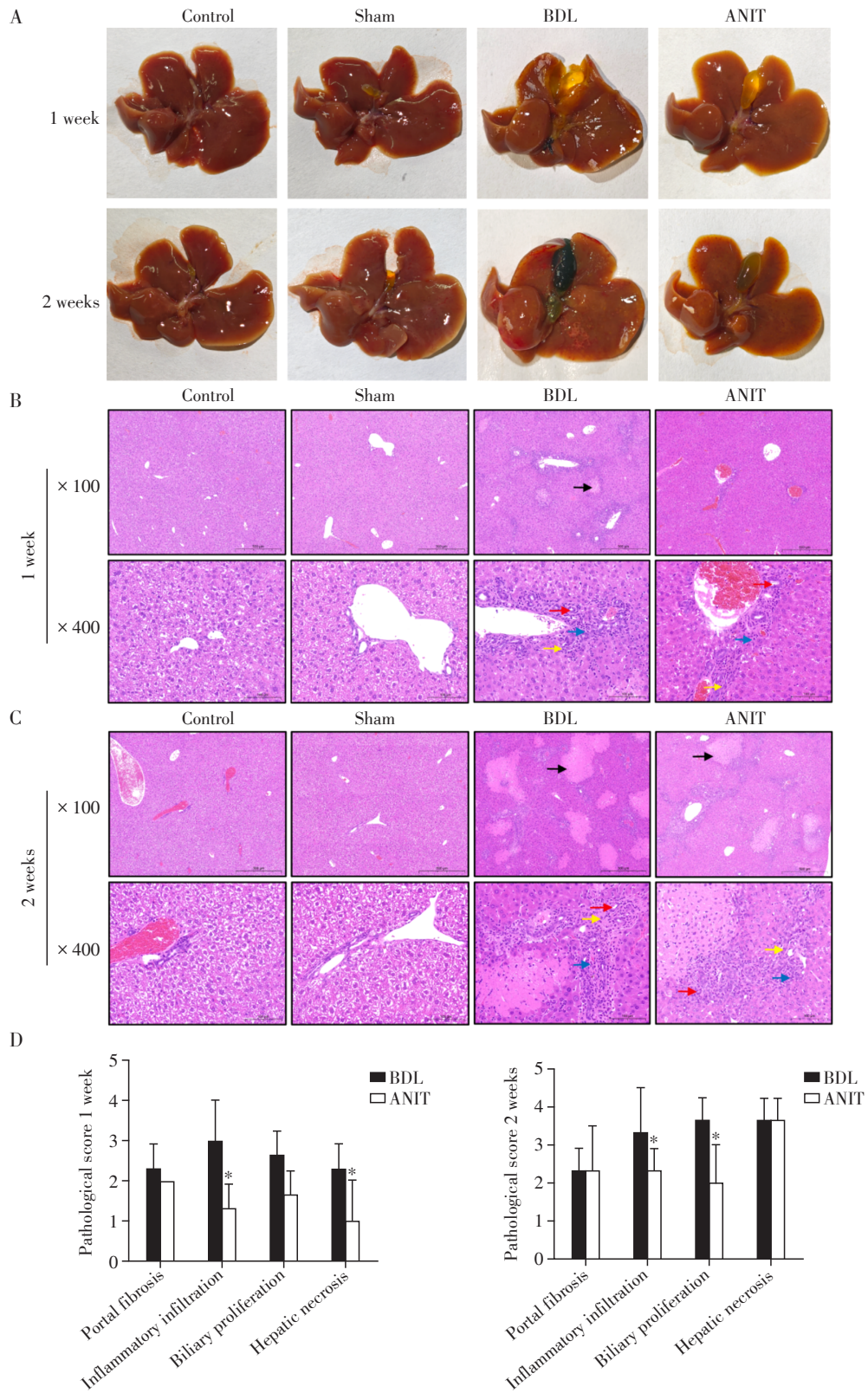
2.2.1 肝脏形态学及病理学对比

在早期(1周)及晚期(2周)解剖两种模型小鼠,发现BDL组小鼠早期肝脏质地较硬,色泽暗淡,伴胆囊充盈明显,部分出现肝脏明显变大,晚期肝脏硬化加重;ANIT组小鼠早期肝脏可见点状损伤,部分质地较硬,无胆囊充盈,晚期坏死灶增多(图2A)。进一步的HE染色发现,早期BDL组小鼠汇管区中度纤维化(黄色箭头),炎症细胞浸润(蓝色箭头),胆管增多(红色箭头),有较多的局灶性肝细胞坏死(黑色箭头);早期ANIT组小鼠肝脏中央静脉和汇管区见有炎症细胞浸润,汇管区结缔组织增生和胆管增多(图2B)。晚期BDL组的小鼠肝组织中,汇管区中度纤维化,在汇管区浸润的炎症细胞较多,伴胆管增多,有大小不等的肝细胞坏死灶。

晚期ANIT组小鼠肝内汇管区结缔组织增生明显,炎症细胞中度浸润,胆管增加,可见弥散性大小不一坏死灶(图2C)。对两组肝脏汇管区纤维化、炎症细胞浸润、胆管增生和坏死结节进行评分,BDL组早期坏死结节及炎症细胞浸润较ANIT组明显($P < 0.05$);晚期两种模型小鼠评分均上升,BDL组胆管增生较ANIT组更明显($P < 0.05$),其他各项评分与BDL组接近($P > 0.05$,图2D)。

2.2.2 肝脏功能血清学对比

收集各组小鼠早期及晚期血清进行分析,早期两组模型小鼠AST、ALT水平均较对照组明显上升($P < 0.05$),两组间差异无统计学意义($P > 0.05$),但BDL组ALP与TBIL水平升高较ANIT组明显($P < 0.05$,图3A);炎症因子检测显示,早期两组模型小鼠IL-1 β 、IL-6和MCP-1水平较对照组明显上升



A: Gross morphological features of liver tissues across experimental groups. B, C: H&E staining of hepatic tissues at 1 week and 2 weeks intervals post-induction (black arrows: necrotic foci; yellow arrows: portal connective tissue hyperplasia; blue arrows: inflammatory cell infiltration; red arrows: ductular proliferation; $\times 100$, $\times 400$). D: Semiquantitative assessment of liver injury severity in the two experimental models. Compared to the ANIT group, $^*P < 0.05$ ($n=6$).

图2 BDL和ANIT模型肝脏病变的组织病理学对比分析

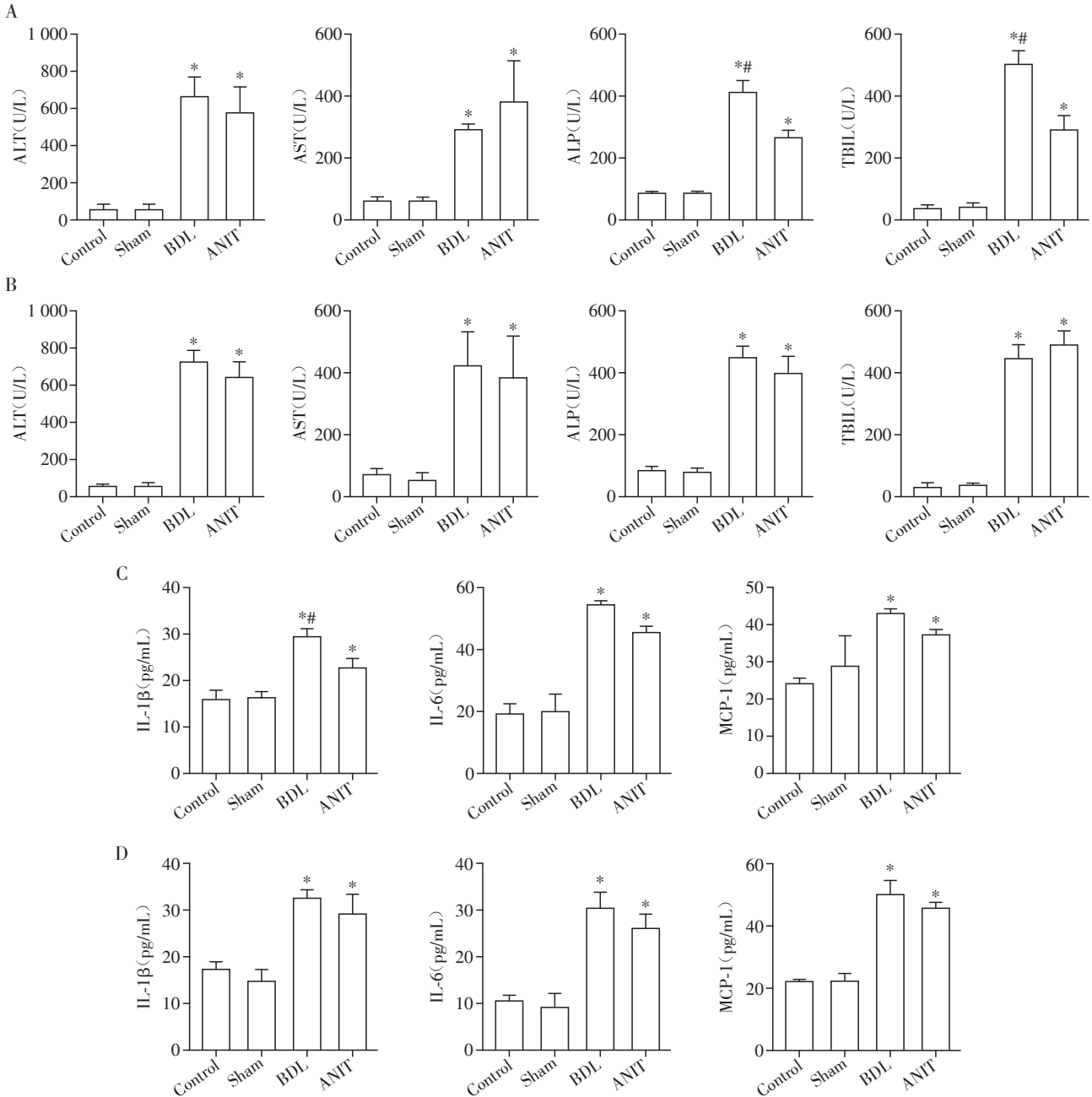
Figure 2 Comparative histopathological analysis of hepatic lesions in BDL and ANIT models

($P < 0.05$), 其中BDL组IL-1 β 水平升高较ANIT组明显($P < 0.05$, 图3C)。晚期两组模型小鼠AST、ALT水平仍明显升高($P < 0.05$), 两组之间差异无统计学意义($P > 0.05$); 但ANIT组小鼠血清中ALP、TBIL与炎症因子(IL-1 β 、IL-6和MCP-1)水平升高迅速($P < 0.05$), 接近于BDL组水平($P > 0.05$, 图3B、D)。

3 SCFA在两种小鼠模型中的治疗效果对比

3.1 小鼠表现对比

在分别进行BDL以及ANIT造模后给予小鼠SCFA, 治疗2周后BDL+SCFA组小鼠黄疸继续加深, 体重仍持续下降, 而ANIT+SCFA组初始有体重



A: Expression levels of early-phase serum biochemical parameters: ALT, AST, ALP, and TBIL at the first week. B: Expression levels of late-phase serum biochemical parameters: ALT, AST, ALP, and TBIL at the second week. C: Expression levels of early-phase inflammatory mediators: IL-1 β , IL-6, and MCP-1 at the first week. D: Expression levels of late-phase inflammatory mediators: IL-1 β , IL-6, and MCP-1 at the second week. Compared to the control group, * $P < 0.05$; compared to the ANIT group, # $P < 0.05$ ($n=6$).

图3 胆汁淤积模型小鼠早晚期血清生化指标和炎症细胞因子水平变化

Figure 3 Alterations in serum biochemical markers and inflammatory cytokine levels during the early and late phases of cholestatic models in mice

下降表现, 后续逐渐升高, 2周时体重较 ANIT 组差异有统计学意义 ($P < 0.05$, 图 4A), 黄疸未进一步加深。

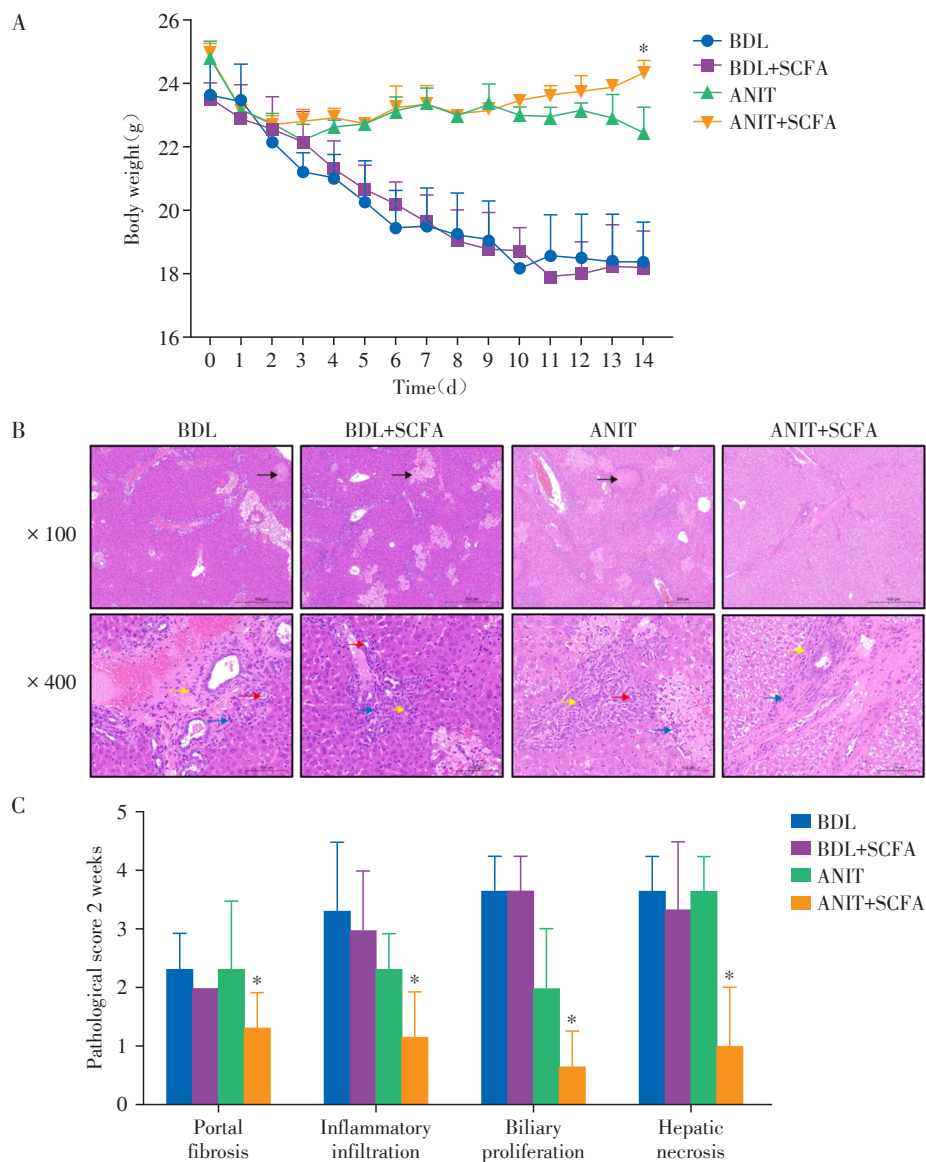
3.2 肝脏病理改变对比

SCFA 治疗 2 周后, 各组小鼠肝脏 HE 染色显示, BDL+SCFA 组小鼠的肝脏损伤明显, 肝细胞坏死, 炎症细胞浸润和胆管增生仍较为显著; ANIT+SCFA 组小鼠肝细胞损伤和炎症细胞浸润显著减少, 有轻度的胆管增生(图 4B)。通过对 4 组小鼠肝脏汇管区纤维化、炎性细胞浸润、胆管增生和坏死结节进行评分, BDL+SCFA 组小鼠病理评分无明显改变, 而 ANIT+SCFA 组小鼠各项病理评分较 ANIT 组明显下

降 ($P < 0.05$, 图 4C), 呈改善趋势。

3.3 血清学改变对比

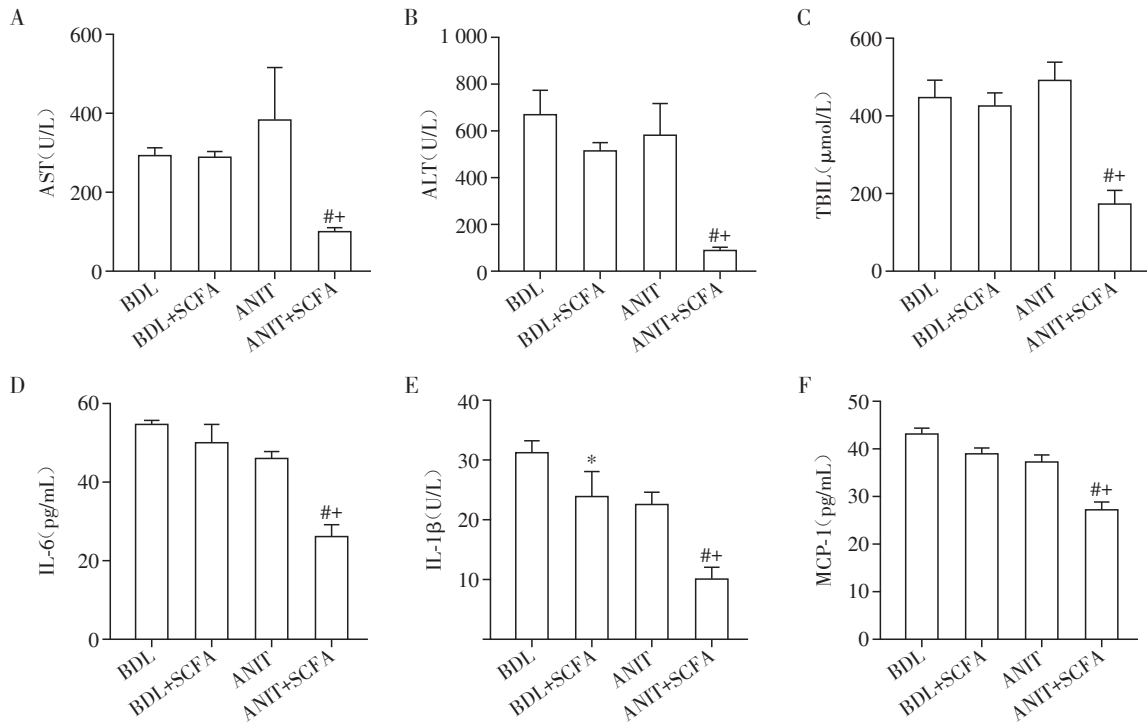
BDL+SCFA 组小鼠的 ALT、AST 和 TBIL 水平较模型组无明显变化 ($P > 0.05$), ANIT+SCFA 组小鼠的 ALT、AST 和 TBIL 水平较 ANIT 组显著下降 ($P < 0.05$, 图 5A~C)。小鼠血清炎症因子检测表明, BDL+SCFA 组中的 IL-1 β 水平较 BDL 组下降明显 ($P < 0.05$), 而 IL-6 和 MCP-1 水平较 BDL 组下降不明显 ($P > 0.05$); 而 SCFA 显著降低了 ANIT 模型小鼠血清中的 IL-1 β 、IL-6 和 MCP-1 水平 ($P < 0.05$, 图 5D~F)。



A: Body weight trajectories across experimental groups. B: Hepatic histopathological features by H&E staining (black arrows: necrotic foci; yellow arrows: portal tract fibrosis; blue arrows: inflammatory cell infiltration; red arrows: bile duct proliferation). C: Semiquantitative assessment of liver injury severity. Compared to the ANIT group, * $P < 0.05$ ($n=6$).

图 4 SCFA 对胆汁淤积模型体重及肝组织病理学特征的改善作用

Figure 4 Therapeutic effects of SCFA on body weight dynamics and hepatic injury in cholestatic models



A-C: Comparative analysis of AST(A), ALT(B) and TBIL concentrations(C) across experimental groups. D-F: Pro-inflammatory cytokine expression levels across experimental groups. Compared with the BDL group, * $P < 0.05$; compared with the ANIT group, # $P < 0.05$; compared to the BDL+SCFA group, ^{#+} $P < 0.05$ ($n=6$).

图5 SCFA对胆汁淤积模型中肝脏损伤生物标志物和全身炎症的调节作用

Figure 5 Modulatory effects of SCFA on hepatic injury biomarkers and systemic inflammation in cholestatic models

4 讨论

胆汁淤积性肝损伤的发病机制复杂,治疗手段有限以及预后不良,是临床的一个棘手问题,也是目前研究的难点与热点。胆汁淤积性肝损伤病因多样,可由多种肝内外病变引起^[5]。为研究胆汁淤积性肝损伤,发明了众多小鼠动物模型,如手术(胆管结扎术)、化学诱导(3,5-二乙氧基羰基-1,4-二氢可力丁、ANIT等)、病毒感染和基因编辑等^[11,22]。这些模型主要用于研究胆汁淤积性肝损伤的机制,并探索新的治疗药物及方法^[9,23]。BDL模型与ANIT模型是其中两种常用的诱导胆汁淤积性肝损伤的模型,本研究通过比较这两种胆汁淤积小鼠模型在外观表现、肝损伤特征、血清学指标各方面的差异,并使用SCFA作为治疗药物,观察两种模型肝损伤的缓解情况,探索两种模型在胆汁淤积性肝损伤实验中的应用范围。

首先是外观表现上,BDL组小鼠起病急,早期即出现体重明显下降且呈现持续性,黄疸出现早且明显,毛发枯燥,后期出现严重黄疸;ANIT组早期体重轻度下降,后期体重变化不明显,黄疸出现迟,后

期逐渐加重。肝组织大体与形态学中两种模型有共同表现,包括部分肝脏硬化、肝细胞坏死、汇管区纤维化、炎性细胞浸润以及胆管增生。但BDL和ANIT模型亦有差异,BDL组早期就出现这些表现,小鼠肝脏硬化更严重,HE染色也显示较多肝细胞坏死灶、大量炎症细胞浸润和胆管增生;ANIT组早期表现为肝坏死灶较少、汇管区结缔组织增生、中度的炎性细胞浸润和胆管增生,晚期肝坏死灶增多,炎症细胞浸润加重。两组小鼠晚期病理评分均高于早期,早期ANIT坏死灶和炎性细胞浸润的病理评分低于BDL组,晚期各项病理评分与BDL组接近。

在血清学指标方面,BDL组小鼠的ALT、AST、ALP和TBIL水平均在早期显著升高,反映出胆管阻塞和胆汁淤积的早期反应。ANIT组小鼠的ALT、AST水平早期明显升高,ALP和TBIL的升高幅度则较小,表明该模型的早期胆汁淤积程度相对较轻。晚期两组小鼠ALP与TBIL水平均明显升高,说明ANIT组胆汁淤积持续加重。血清炎症因子的变化显示,早期BDL组炎症因子水平较ANIT升高明显;BDL组和ANIT组小鼠的炎症反应在晚期均明显增

强,IL-1 β 、IL-6和MCP-1的水平明显升高,这与既往研究相符^[24]。上述指标反映了BDL模型早期出现严重的胆汁淤积性肝损伤,ANIT模型则呈现逐渐加重的胆汁淤积性肝损伤。

本课题组前期研究发现SCFA可以改善对乙酰氨基酚诱导的急性肝损伤,并减少了肝脏中炎症反应^[20],此外,多项研究证实SCFA有助于肠道或肝脏损伤的改善^[25-26],基于以上研究背景,本研究使用SCFA作为治疗药物,系统探讨其在不同类型胆汁淤积性肝损伤中的治疗效果。研究发现SCFA在不同模型中表现出显著的疗效差异。在BDL模型中,SCFA治疗2周对BDL组的黄疸、体重下降、肝脏血清学指标及炎症指标改善不明显,这表明以BDL模型为代表的急性机械性胆汁淤积性肝损伤中SCFA类药物治疗效果有限。而在ANIT模型中,SCFA展现出了显著的治疗效果。SCFA不仅显著降低了ALT、AST和TBIL的水平,还减少了肝脏病理损伤程度、炎症细胞浸润和胆管增生。且SCFA能够显著降低ANIT模型小鼠血清中的IL-1 β 、IL-6和MCP-1水平。这表明以ANIT模型为代表的慢性化学性胆汁淤积性肝损伤中SCFA可能有治疗效果。

综上所述,BDL模型与ANIT模型有部分共性表现,如体重下降、黄疸出现、肝细胞坏死、汇管区纤维化、炎症细胞浸润等;但BDL模型起病急,黄疸出现早且明显,肝损伤严重,适用于研究急性胆汁淤积性肝损伤,如急性药物性肝损伤、急性病毒性肝炎和胆道梗阻疾病等;ANIT模型起病缓慢,黄疸以及肝损伤进行性加重,更适合模拟慢性胆汁淤积性肝损伤,比如PSC、慢性药物性肝损伤、慢性病毒性肝炎和肝硬化等。

利益冲突声明:

所有作者声明无利益冲突。

Conflict of Interests:

All the authors declared no conflicts of interest.

作者贡献声明:

路寒负责实施研究、分析数据和起草文章;张雪飞负责采集数据和统计分析;孙学伟负责工作及技术支持;张若男和张昕蕊帮助造模;张明燕和唐成亮收集样本;杨展负责研究指导;朱进负责研究经费支持;杨晓俊负责实验设计、审阅论文和研究指导。

Author's Contributions:

LU Han was responsible for conducting the study, analyzing data, and drafting the manuscript. ZHANG Xuefei was in charge of data collection and statistical analysis. SUN Xuewei provided technical and project support. ZHANG Ruonan and

ZHANG Xinrui assisted with model induction. ZHANG Mingyan and TANG Chengliang collected samples. YANG Zhan supervised the study. ZHU Jin provided financial support. YANG Xiaojun was responsible for experimental design, manuscript review, and study supervision.

[参考文献]

- [1] WOOLBRIGHT B L. Inflammation: cause or consequence of chronic cholestatic liver injury[J]. *Food Chem Toxicol*, 2020, 137: 111133
- [2] CHEN Y, HU Q C, ZHANG W W, et al. Chidan Tuihuang granule modulates gut microbiota to influence NOD1/RIPK2 pathway in cholestatic liver injury recovery [J]. *Phytomedicine*, 2024, 135: 156164
- [3] WEI C L, QIU J, WU Y Y, et al. Promising traditional Chinese medicine for the treatment of cholestatic liver disease process(cholestasis, hepatitis, liver fibrosis, liver cirrhosis)[J]. *J Ethnopharmacol*, 2022, 297: 115550
- [4] FU K, LI Y Z, DAI S, et al. Exploration of the molecular basis of Forsythia fruit in the prevention and treatment of cholestatic liver injury through network pharmacology and molecular docking[J]. *Nutrients*, 2023, 15(9): 2065
- [5] WU R, ZOU X P, ZHANG B. A rare cause of obstructive jaundice[J]. *Gastroenterology*, 2023, 164(6): e5-e8
- [6] LÜT T, CHEN S, LI M, et al. Regional variation and temporal trend of primary biliary cholangitis epidemiology: a systematic review and meta-analysis [J]. *J Gastroenterol Hepatol*, 2021, 36(6): 1423-1434
- [7] LEE Y M, KAPLAN M M. The natural history of PBC: has it changed?[J]. *Semin Liver Dis*, 2005, 25(3): 321-326
- [8] LAZARIDIS K N, LARUSSO N F. Primary sclerosing cholangitis [J]. *N Engl J Med*, 2016, 375(12): 1161-1170
- [9] GIJBELS E, PIETERS A, DE MUYNCK K, et al. Rodent models of cholestatic liver disease: a practical guide for translational research [J]. *Liver Int*, 2021, 41(4): 656-682
- [10] 董 跨,唐莹莹,蒋嘉瑞,等.泽泻改善胆管结扎致小鼠肝纤维化的药效与机制研究[J/OL]. *药学报*, [2025-03-18] DOI: <https://doi.org/10.16438/j.0513-4870.2024-1104>
DONG K, TANG Y Y, JIANG J R, et al. Study on the hepatoprotective effects and mechanism of Alismatis Rhizoma extracts in bile duct ligation-induced liver fibrosis in mice [J/OL]. *Acta Pharmaceutica Sinica*, [2025-03-18] DOI: <https://doi.org/10.16438/j.0513-4870.2024-1104>
- [11] TAG C G, SAUER-LEHNEN S, WEISKIRCHEN S, et al. Bile duct ligation in mice: induction of inflammatory liver

- injury and fibrosis by obstructive cholestasis [J]. *J Vis Exp*, 2015(96): 52438
- [12] POLLHEIMER M J, TRAUNER M, FICKERT P. Will we ever model PSC?-"it's hard to be a PSC model!" [J]. *Clin Res Hepatol Gastroenterol*, 2011, 35(12): 792-804
- [13] VAN CAMPENHOUT S, VAN VLIERBERGHE H, DE- VISSCHER L. Common bile duct ligation as model for secondary biliary cirrhosis [J]. *Methods Mol Biol*, 2019, 1981: 237-247
- [14] CARPENTER-DEYO L, MARCHAND D H, JEAN P A, et al. Involvement of glutathione in 1-naphthylisothiocyanate (ANIT) metabolism and toxicity to isolated hepatocytes [J]. *Biochem Pharmacol*, 1991, 42(11): 2171-2180
- [15] ASSIS D N, BOWLUS C L. Recent advances in the management of primary sclerosing cholangitis [J]. *Clin Gastroenterol Hepatol*, 2023, 21(8): 2065-2075
- [16] RAUF A, KHALIL A A, RAHMAN U U, et al. Recent advances in the therapeutic application of short-chain fatty acids (SCFAs): an updated review [J]. *Crit Rev Food Sci Nutr*, 2022, 62(22): 6034-6054
- [17] ZHANG S M, ZHAO J W, XIE F, et al. Dietary fiber-derived short-chain fatty acids: a potential therapeutic target to alleviate obesity-related nonalcoholic fatty liver disease [J]. *Obes Rev*, 2021, 22(11): e13316
- [18] SHASHNI B, TAJIKA Y, IKEDA Y, et al. Self-assembling polymer-based short chain fatty acid prodrugs ameliorate non-alcoholic steatohepatitis and liver fibrosis [J]. *Biomaterials*, 2023, 295: 122047
- [19] AWONIYI M, WANG J, NGO B, et al. Protective and aggressive bacterial subsets and metabolites modify hepatobiliary inflammation and fibrosis in a murine model of PSC [J]. *Gut*, 2023, 72(4): 671-685
- [20] SUN X W, CUI Q, NI J, et al. Gut microbiota mediates the therapeutic effect of monoclonal anti-TLR4 antibody on acetaminophen-induced acute liver injury in mice [J]. *Microbiol Spectr*, 2022, 10(3): e0064722
- [21] ISHAK K, BAPTISTA A, BIANCHI L, et al. Histological grading and staging of chronic hepatitis [J]. *J Hepatol*, 1995, 22(6): 696-699
- [22] LI J, ZHU X Y, ZHANG M H, et al. Limb expression 1-like (LIX1L) protein promotes cholestatic liver injury by regulating bile acid metabolism [J]. *J Hepatol*, 2021, 75(2): 400-413
- [23] WANG M Q, ZHANG K H, LIU F L, et al. Wedelolactone alleviates cholestatic liver injury by regulating FXR-bile acid-NF- κ B/NRF2 axis to reduce bile acid accumulation and its subsequent inflammation and oxidative stress [J]. *Phytomedicine*, 2024, 122: 155124
- [24] LABIANO I, AGIRRE-LIZASO A, OLAIZOLA P, et al. TREM-2 plays a protective role in cholestasis by acting as a negative regulator of inflammation [J]. *J Hepatol*, 2022, 77(4): 991-1004
- [25] WANG Z, ZHANG X X, ZHU L L, et al. Inulin alleviates inflammation of alcoholic liver disease via SCFAs-inducing suppression of M1 and facilitation of M2 macrophages in mice [J]. *Int Immunopharmacol*, 2020, 78: 106062
- [26] WANG W, ZHAO X, MA Y, et al. Alleviating effect of *Lactocaseibacillus rhamnosus* 1.0320 combined with dihydromyricetin on acute alcohol exposure-induced hepatic impairment: based on short-chain fatty acids and adenosine 5'-monophosphate-activated protein kinase-mediated lipid metabolism signaling pathway [J]. *J Agric Food Chem*, 2023, 71(12): 4837-4850

[收稿日期] 2025-01-22

(本文编辑:戴王娟)